Direct Measurement of the Hyperfine Structure of the Ground State Positronium using High Power Sub-THz Radiation

Takayuki Yamazaki[1], Akira Miyazaki[1], Taikan Suehara[1], Toshio Namba[1], Shoji Asai[1], Tomio Kobayashi[1], Haruo Saito[2], Toshitaka Idehara[3], Isamu Ogawa[3], and Svilen Sabchevski[4]

[1]*Department of Physics, Graduate School of Science, and International Center for Elementary Particle Physics, University of Tokyo, Japan*

[2]*Graduate School of Arts and Sciences, University of Tokyo, Japan*

[3]*Research Center for Development of Far-Infrared Region, University of Fukui, Japan*

[4]*Bulgarian Academy of Sciences, Bulgaria*

yamazaki@icepp.s.u-tokyo.ac.jp

Abstract

Positronium (Ps) is a good target to study Quantum Electrodynamics (QED) precisely. A large discrepancy (3.9 σ, 15 ppm) is found recently between the measured and the theoretical value of the hyperfine structure of the ground state positronium (Ps-HFS, 203.4 GHz). It might be due to the contribution of new physics or common systematic uncertainties in the previous indirect measurements using Zeeman effect. In order to perform a direct measurement of Ps-HFS, we develop a new optical system which consists of a gyrotron as a radiation source and a Fabry-Pérot resonant cavity to accumulate high power ($\sim$ 10 kW) sub-THz (202.9 GHz) radiation. The transition between Ps-HFS has been clearly observed with 5.4 σ confidence level for the first time. We plan to measure Ps-HFS with an accuracy of O(100 ppm) in a year by repeating transition measurements at five frequency points around 203.4 GHz.

1. Introduction

Positronium (Ps), a bound state of an electron and a positron, is a purely leptonic system and is a good target to study Quantum Electrodynamics (QED) in bound state. The triplet (1^3S_1) state of Ps is called ortho-positronium (o-Ps) and mainly decays into three γ rays with long lifetime of 142 ns [1–3]. On the other hand, the singlet (1^1S_0) state of Ps is called para-positronium (p-Ps) and mainly decays into two γ rays promptly (lifetime is 125 ps [4]). The energy level of the ground state o-Ps is higher than that of the ground state p-Ps because of the spin-spin interaction. The difference is called the hyperfine structure of the ground state positronium (Ps-HFS). The Ps-HFS is significantly large (203.4 GHz) compared to the hyperfine structure of the hydrogen atom (about 1.4 GHz).

Precise measurement of Ps-HFS gives the direct information on QED, especially in the bound state. The precise measurements have been performed in 1970's and 1980's, whose results are shown in Fig. 1 with the theoretical value. All previous measurements of the Ps-HFS employed static magnetic field (about 1 T) and the Ps-HFS has been measured indirectly using Zeeman splitting (about 3 GHz). These results are consistent with each other, and the combined value of the most accurate two results [5, 6] is 203.388 65(67) GHz (3.3 ppm). This combined value is shown with the green band.

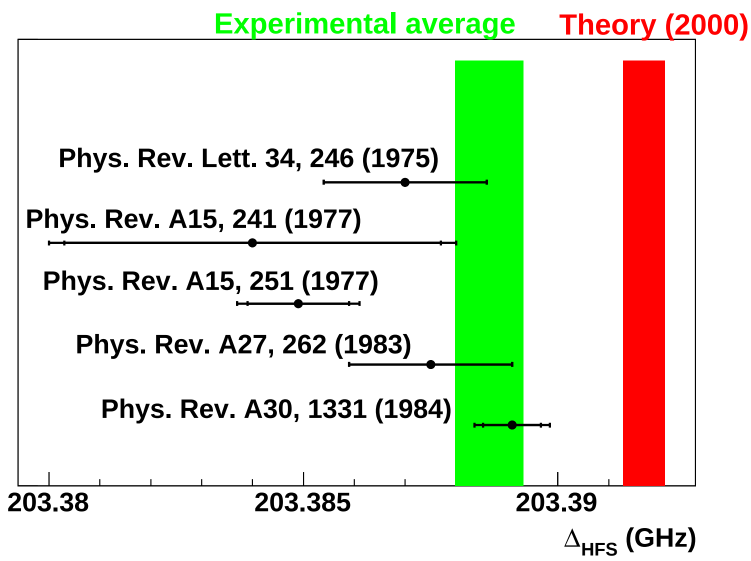

Figure 1: Historical plot of the Ps-HFS value. Points with error bars show the experimental results with references. The green and red bands show the average of the measured values (the average of the latest two results) and the theoretical calculation up to $O(\alpha^3 \log \alpha^{-1})$, respectively.

New method to calculate the higher order corrections up to $O(\alpha^3 \log \alpha^{-1})$ for the bound state is established in 2000 [7]. The QED prediction is 203.391 69(41) GHz (2 ppm) shown with the red band. There is a large discrepancy (3.9 σ, 15 ppm) between the measured and the theoretical value. It is very important to measure the Ps-HFS again with a method totally different from the previous experiments since non-uniformity of the static magnetic field is the most significant systematic error in the previous experiments.

Direct measurement of the Ps-HFS is free from systematic uncertainty of the static magnetic field, but it has never been performed because the rate of spontaneous emission (or Einstein's A coefficient $A = 3.37 \times 10^{-8}$ [s^{-1}]) is 14 orders of magnitude smaller than the decay rate of o-Ps ($\lambda_{\mathrm{o-Ps}} = 7.0401(7) \times 10^6$ [s^{-1}] [3]).

High power sub-THz radiation is necessary to cause sufficient amount of stimulated emission but there was no high power radiation source so far, therefore even the hyperfine transition itself has not yet been observed. However, the recent development of the gyrotron [8], which is a novel high power radiation source for sub-THz to THz region, changes the situation. Its output is monochromatic, the power is high, and it can operate in continuous wave (CW). Although the direct output power of the gyrotron is not high enough to cause sufficient amount of the hyperfine transition between Ps-HFS, we can achieve it (~ 10 kW) by accumulating the output radiation in a Fabry-Pérot resonant cavity. The first target of our experiment is to observe the hyperfine transition for the first time using the new optical system, and the result is reported in this paper.

2. Experimental Setup

2.1 Gyrotron

Figure 2 shows the schematic of the experimental setup (left) and the picture of the gyrotron named Gyrotron FU CW V (right), which is dedicated to the first phase of direct Ps-HFS measurement. Gyrotron FU CW V is stably operated at $f = 202.9$ GHz (TE_{03} mode) for on-resonance measurement, and the peak power is about 300 W (20 Hz, duty 30 %). TE_{02} mode ($f = 140$ GHz) is also used for off-resonance measurement. We stabilize the gyrotron output power within 10 % fluctuation by controlling the heater voltage of the electron gun during data taking of transition measurement.

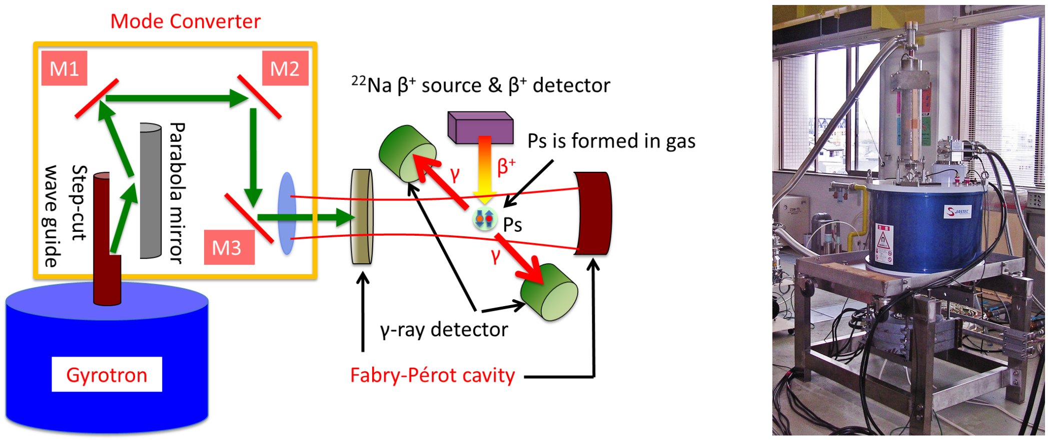

Figure 2: The schematic of the experimental setup (left) and the picture of Gyrotron FU CW V (right).

2.2 Mode Converter

The output power of the gyrotron is high (~ 300 W) but not enough to observe the hyperfine transition of Ps. The radiation have to be accumulated in a Fabry-Pérot cavity, but the wave mode of the Fabry-Pérot cavity is a Gaussian beam, which is completely different from TE_{0n} mode. As a result, the raw output of the gyrotron cannot be coupled with the Fabry-Pérot cavity at all. A mode converter to convert the gyrotron output into a Gaussian beam is necessary.

Figure 3 shows a picture of the mode converter (left). Its main component is the step-cut waveguide made of copper and the Vlasov antenna, which is a large parabolic mirror made of aluminum. It converts TE_{0n} mode to a plain wave (or bi-Gaussian beam) geometrically by matching the center of the step-cut waveguide and the focus point of the Vlasov antenna [9]. The following two mirrors shape the bi-Gaussian beam into a Gaussian beam.

Figure 3 also shows the space distribution measured by taking a picture of PVC sheet exposed to radiation by an infrared camera. Top and bottom right figure are power profiles before and after the mode converter, respectively. The conversion efficiency is not good (28 ± 2 %) because the wave mode of the gyrotron output is not perfect TE_{0n} wave mode.

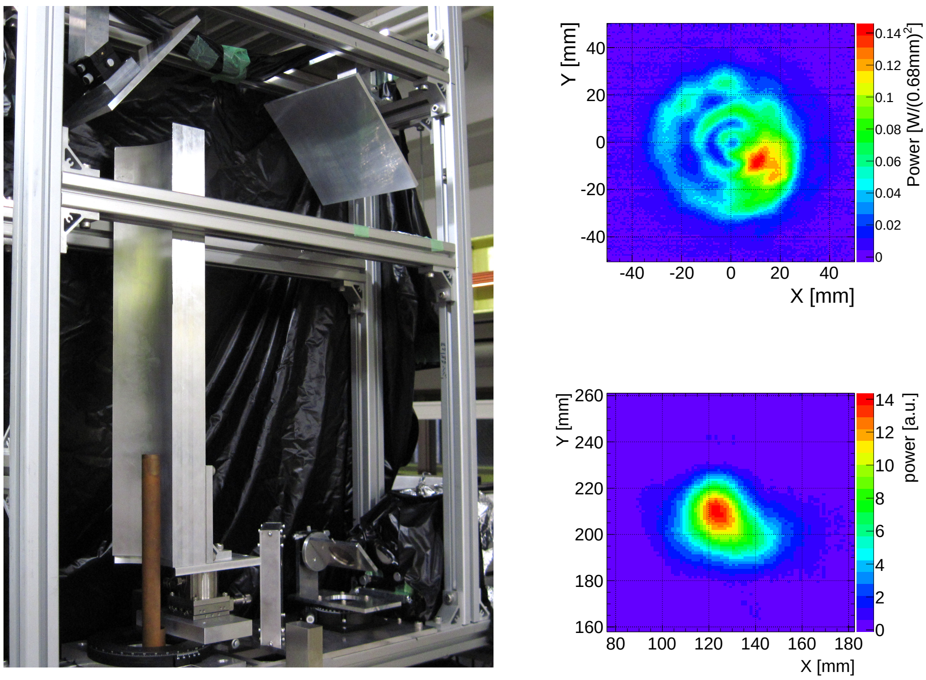

Figure 3: A picture of the mode converter (left) and Top and bottom figure are power profiles before and after the mode converter, respectively (right).

2.3 Fabry-Pérot Cavity

A Fabry-Pérot cavity is made with a gold mesh plain mirror ($\phi = 50$ mm) and a Cu concave mirror ($\phi = 50$ mm, curvature $= 300$ mm). The incident Gaussian beam is resonant with the cavity when the cavity length (136 mm) is equal to the half-integer multiple of λ, where λ is the radiation wavelength (1.5 mm). The cavity length is controlled by moving the Cu concave mirror mounted on an X-axis stage.

The Au mesh plain mirror is a key component in order to obtain high gain resonator. The Au mesh is made on a SiO_2 plate using conventional photolithography and liftoff technique. Figure 4 shows a picture of the Au mesh plain mirror (left). The line width is 200 μm and the line separation is 160 μm, which are designed to obtain high reflectivity and reasonable transmittance. Its simulated reflectivity is $R = 99.38$ % and the transmittance is $T = 0.39$ % for 202.9 GHz radiation.

The right figure of Fig. 4 shows the accumulated power, which is estimated from the transmitted power monitored with a pyroelectric detector while changing cavity length of the Fabry-Pérot cavity. FWHM of the resonance peak is 1.19(6) μm, which corresponds to the finesse $\mathcal{F} = 623 \pm 29$. The accumulated power reaches ~ 10 kW.

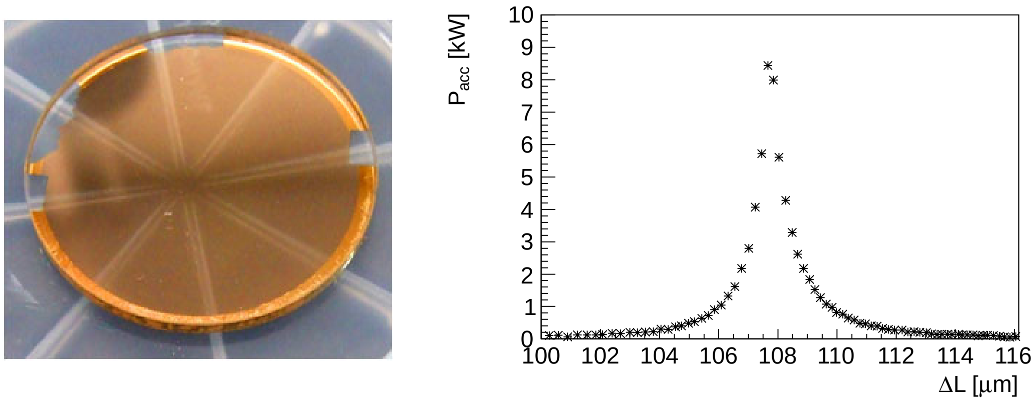

Figure 4: The left figure shows a picture of the Au mesh plain mirror. The right figure shows the accumulated power of the Fabry-Pérot cavity.

2.4 Ps assembly and γ-ray Detectors

Figure 5 shows a schematic of Ps assembly and γ-ray detectors (left). A positron emitted from a ^{22}Na positron source (780 kBq), and a thin (100 μm) plastic scintillator detects the emission. About 5 % of the positrons are tagged by the plastic scintillator and stop in the gas, and positroniums are formed. The Ps assembly and the Fabry-Pérot cavity are in a gas chamber (Fig. 5 (right)). High power sub-THz radiation in the Fabry-Pérot cavity causes the hyperfine transition from o-Ps to p-Ps, and as a result, the number of 2γ decay events increases. The γ rays are detected by surrounding γ-ray detectors. We use four $LaBr_3$(Ce) crystal scintillators because of its good energy resolution (FWHM = 4 % at 511 keV) and fast time response (decay constant is 16 ns). These are advantages for tagging monochromatic 511 keV gamma rays and avoiding pileups.

3. Analysis and Result

Four RUNs have been performed. RUN I, III and IV use 202.9 GHz radiation (TE_{03} mode) and they are different in power accumulated in the Fabry-Pérot cavity. RUN I is the highest power RUN and the accumulated power is 11.0 kW (peak energy density of 0.28 J/m^3 at the center of the Fabry-Pérot cavity) in the average during the data acquisition (DAQ). RUN II is the off-resonance data and uses 140 GHz radiation (TE_{02} mode) to check systematic uncertainties. The DAQ is triggered when back-to-back γ-ray signals from the $LaBr_3$(Ce) scintillators are coincident within 40ns and then when this coincidence is within -100 ns to 1100 ns of the timing of the plastic scintillator signal. The trigger rate is about 1 kHz.

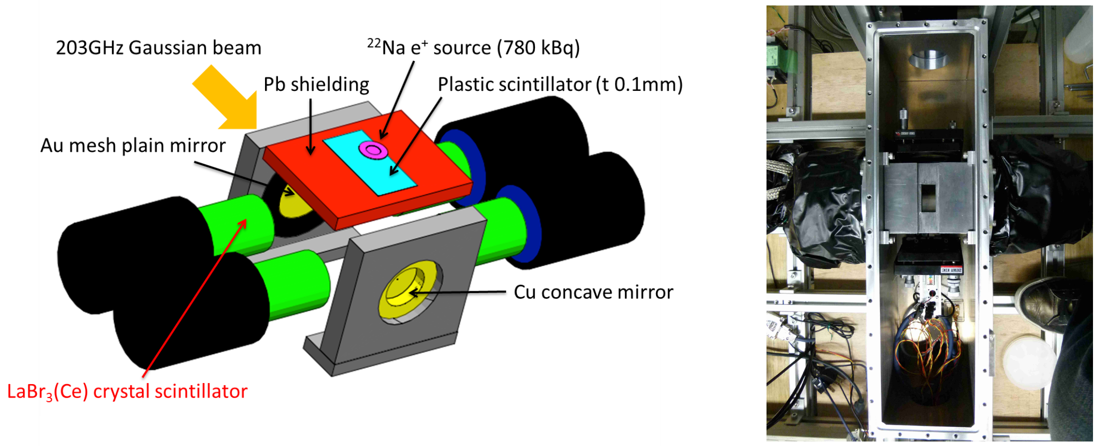

Figure 5: The left figure shows the schematic of the Ps assembly and γ-ray detectors. The right figure is a picture of a gas chamber in which Ps assembly and the Fabry-Pérot cavity are installed.

The transition signals are the events that p-Ps ($\tau = 125$ ps) transited from o-Ps ($\tau = 142$ ns) decays into two back-to-back monochromatic (511 keV) γ rays. Therefore the transition signals have long lifetime of o-Ps and decay into two back-to-back monochromatic (511 keV) γ rays.

Figure 6 shows the time difference between the plastic scintillator and the coincidence signal of the $LaBr_3$(Ce) scintillators. A sharp peak, called as the prompt peak is observed at $t = 0$, where e^+ annihilations and p-Ps decays are dominant. The time region after the prompt peak is dominated by the o-Ps events and forms the exponential decay curve. The flat time spectrum far beyond the prompt peak is dominated by the accidental events. The γ-ray hit of the accidental event is not correlated with the triggered e^+ hit. A time window from 50 ns to 350 ns is required to enhance o-Ps lifetime events and improves S/N. In addition, accidental rejection cut is applied to suppress accidental background. In the case of accidental events, there is another plastic scintillator hit at the timing of γ-ray hit. The energy deposit on the plastic scintillator is measured with long and short gate at the same time. If the long gate energy is larger than the short gate energy, the event is vetoed. The black and the red line show before and after the accidental rejection cut, respectively.

In Fig. 7, the left figure shows γ-ray energy spectra of “beam ON” (red) and “beam OFF” (black) data after all event selections are applied. The data taken during “beam OFF” period in the pulse beam are used to estimate background. The 511 keV peak of “beam OFF” spectrum consists of pick-off annihilation and 3γ decay of o-Ps. When the hyperfine transition of the ground state Ps occurs, the number of events at 511 keV peak increases. Transition signal is clearly observed and the signal rate is $15.1 \pm 2.7(\mathrm{stat.}) \pm^{0.5}_{0.8} (\mathrm{sys.})$ mHz. The systematic errors are summarized in Table 1. This is the first observation of the hyperfine transition between the ground state Ps-HFS with 5.4 σ C.L. The transition probability (or Einstein’s A coefficient)

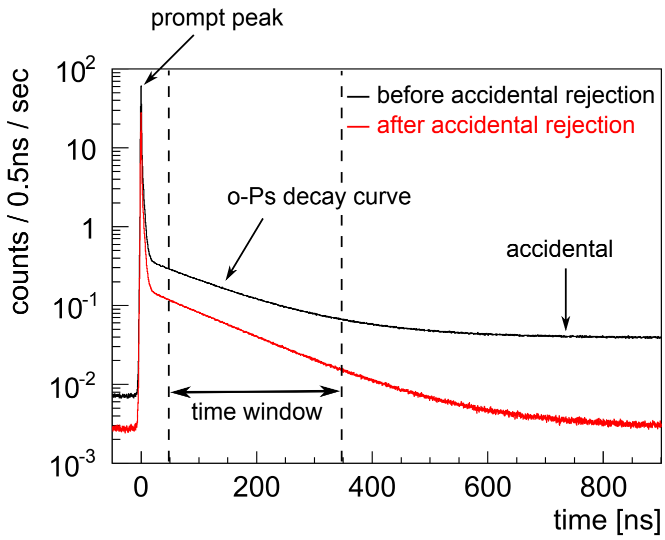

Figure 6: Time difference between the plastic scintillator and the coincidence signal of the $LaBr_3$(Ce) scintillators. The black and the red line show before and after accidental rejection cut, respectively.

estimated from the observed transition rate is $A = 3.1^{+1.6}_{-1.2} \times 10^{-8}$ s^{-1}, which is consistent with theoretical value (3.37×10^{-8} s^{-1}). No excess is observed in off-resonance data (RUN II), and the amount of the transition in on-resonance data is proportional to the accumulated power as shown in the right plot of Fig. 7.

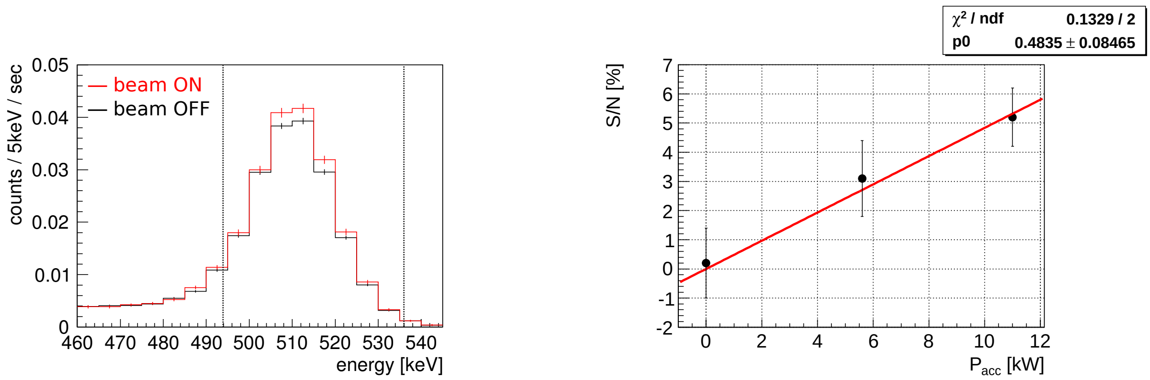

Figure 7: The left figure shows energy spectrum of on-resonance data (RUN I) after all event selections are applied. The red and the black line show "beam ON" and "beam OFF" data, respectively. Transition signal is clearly observed. Moreover, the fraction of the transition signals is proportional to the accumulated power in the Fabry-Pérot cavity (right).

4. Summary and Future Plan

There is a large discrepancy (3.9 σ, 15 ppm) discrepancy between the measured and the theoretical value of Ps-HFS. The most significant common systematic uncertainty of the previous

source	RUN I	RUN II	RUN III	RUN IV
Energy scale and resolution	-0.08 %	$+0.06$ %	-0.11 %	-0.02 %
Ps formation probability	-0.27 %	-0.39 %	$+0.20$ %	-0.13 %
Accidental rejection efficiency	$+0.17$ %	$+0.05$ %	$+0.13$ %	$+0.23$ %
Background normalization	± 0.03 %	± 0.04 %	± 0.04 %	± 0.04 %
Total	${}^{+0.17}_{-0.29}$ %	${}^{+0.08}_{-0.39}$ %	${}^{+0.24}_{-0.12}$ %	${}^{+0.24}_{-0.14}$ %

Table 1: Summary of the systematic errors. The values are percentage of the rate of "beam OFF" events.

indirect measurements is non-uniformity of the static magnetic field to cause Zeeman splitting. It is necessary to measure Ps-HFS again with a different method free from the uncertainty due to static magnetic field. Direct measurement of Ps-HFS has never been performed since high power sub-THz radiation is necessary to cause sufficient amount of stimulated emission. We develop a new optical system consists of the stable gyrotron, the mode converter and the Fabry-Pérot cavity and accumulate high power ($\sim$ 10 kW) sub-THz (202.9 GHz) radiation. With the optical system, the hyperfine transition between Ps-HFS has been observed with 5.4 σ C.L. for the first time.

We plan to perform the first direct measurement of Ps-HFS with an accuracy of O(100 ppm) in a year by repeating transition measurenments at five frequency points around 203.4 GHz. A new gyrotron whose cavity can be quickly replaceable is under development. In the future, we plan to measure Ps-HFS precisely with an accuracy of O(ppm) by using a slow positron beam and creating positronium in vacuum with metal foil.

References

[1] S. Asai *et al.*, Phys. Lett. B **357**, 475 (1995).

[2] O. Jinnouchi *et al.*, Phys. Lett. B **572**, 117 (2003).

[3] Y. Kataoka *et al.*, Phys. Lett. B **671**, 219 (2009).

[4] A. H. Al-Ramadhan and D. W. Gidley, Phys. Rev. Lett. **72**, 1632 (1994).

[5] A. P. Mills, Phys. Rev. A **27**, 262 (1983).

[6] M. W. Ritter *et al.*, Phys. Rev. A **30**, 1331 (1984).

[7] B. A. Kniehl and A. A. Penin, Phys. Rev. Lett. **85**, 5094 (2000).

[8] T. Idehara *et al.*, IEEE Trans. Plasma Sci. **27**, 340 (1999).

[9] I. Ogawa *et al.*, Int. J. Elec. **83**, 5 (1997).